DEVELOPMENT OF SURFACE REFLECTANCE PRODUCTS FROM RESOURCESAT-2 SENSOR DATA AND VALIDATION USING GROUND AND LANSDAT- 8 OLI SURFACE REFLECTANCES

P.K Saritha, V.Keerthi, M.Suresh, T. Radhika, R.N. Anjani, C.V Rao and B. Gopala Krishna
National Remote Sensing Centre, Hyderabad, India, 500625.
Email: saritha_pk, keerthi_v, sureshmanchikanti, radhika_t, anjani_rn, rao_cv, bgk@nrsc.gov.in

KEYWORDS: atmospheric correction, 6S Code, L8-OLI, spectroradiometer

ABSTRACT: Surface Reflectance (SR) products are fundamental inputs for any remote sensing based application. We have implemented an atmospheric correction procedure based on Second Simulation of Satellite Signal in the Solar Spectrum (6S) radiative transfer code for the retrieval of SR products from Resourcesat-2 (RS-2) Advanced Wide Field Sensor (AWiFS) and Linear Imaging Self Scanner (LISS-3) sensor data. The correction is based on lambertian assumption and corrects for aerosol and molecular absorption and scattering effects. The atmospheric characterization parameters are retrieved from MODIS and INSAT climatology products. Coefficients that are required for atmospheric correction are delivered by the 6S code using the above inputs, which are then used to correct RS-2 imagery on a per pixel basis. The surface reflectance product thus generated was evaluated by cross comparison with contemporaneous United States Geological Survey (USGS) provisional Landsat-8 (L8) Operational Land Imager (OLI) SR product and also using ground measured spectral reflectances. Temporal validation over a wide range of target reflectances showed a good correlation between SR retrieved from Landsat-8 and the RS-2 SR product in every band, with R^2 higher than 0.98. Retrieved SR values were also found to be consistent with ground based spectroradiometer measurements. The fact that atmospheric correction do matter is illustrated using NDVI(Normalized Difference Vegetation Index) as an example.

1. INTRODUCTION

The fundamental land surface parameter of interest for any remote sensing based application is surface reflectance products. This is because the retrieval of any biophysical parameter demands for the use of precise surface reflectance products as the input. Moreover surface reflectance products are also necessary to uniformly apply a quantitative remote sensing model or set of classification rules to similarly standardized scenes in different regions or years. So, the accurate conversion from the TOA (Top Of Atmosphere) reflectance to the surface reflectance is an indispensable preprocessing step required for the quantitative utilization of the remote sensing data, and this process is called atmospheric correction (Yong Hu, 2014).

Satellite based measurements of the radiative signature of terrestrial targets are always affected by the atmospheric constituents. Atmospheric effects include molecular and aerosol scattering and absorption by gases, such as water vapor, ozone, oxygen and aerosols. Molecular scattering and absorption by ozone, oxygen and other gases are relatively easy to correct because of the stable concentration in both space and time. The most difficult task is to estimate the distribution of aerosols and water vapor as their concentrations are highly dynamic in both space and time. Aerosols distribution mainly affects the short wave signals, while water vapor affects the long wave signals. A comprehensive overview of the different atmospheric correction methodologies can be found in (Liang, 2004). The atmospheric correction based on radiative transfer code and atmospheric characterization data proves the best for automated large areas application (Diner et al, 2005, Gordon, 1997, Vermote, El Saleous and Justice, 2002). Atmospheric correction is a two step process. In the first step, involves the estimation of atmospheric properties existing at the time satellite over pass. Secondly, a radiative transfer model of the atmosphere is inverted to estimate surface reflectance, accounting for the atmospheric scattering and absorption. Assuming a Lambertian surface and one that is working with near-nadir –viewing optical remotely sensed data, retrieval of surface reflectance is relatively straightforward as long as atmospheric parameters are known.

RS-2 imageries present as a unique data source to monitor the land surface at varied spatial resolution depending on the application. RS-2 imageries have been extensively used for mapping of natural resources and also for the retrieval of various land surface variables. This includes extraction of surface water bodies, snow cover estimation, crop classification, Leaf Area Index (LAI) and Chlorophyll Content Index (CCI) (P K Das et al, 2015).

A procedure has been established to realize surface reflectance products from RS-2 AWIFS and LISS-3 level 2 geo-referenced imageries. The procedure is based on 6S model, which is a widely used operational radiative transfer

model. The correction is based on lambertian assumption and corrects for aerosol and molecular absorption and scattering. This procedure employs MODIS and INSAT climatology data products to arrive at the SR products. Atmospheric input parameters derived from these climatology products include atmospheric water vapor, aerosol optical depth at 550nm (AOD) and ozone. The atmospheric correction tool can generate the correction coefficients based on adaptive grid, using which surface reflectance is derived on a per pixel basis.

The development of a long-term surface reflectance data records requires the development and implementation of methods to verify the quality of the product and also to validate its accuracy. The validation is undertaken in this work by cross comparison with contemporaneous USGS provisional Landsat - 8 OLI SR products. Since OLI surface reflectance products have been validated comprehensively (Vermote et al, 2016), they may be used as a reference to assess the quality of RS-2 surface reflectance products. For each of the four RS-2 LISS-3 and AWiFS multispectral bands, there is a L8 OLI band with a spectral range well within that of the corresponding RS-2 band. The accuracy of the SR products was further assessed by comparison with ground measured spectroradiometer values.

2. DATA USED

2.1 RS-2 AWIFS and LISS -3

RS-2 launched in 2011, was envisaged as a follow on mission to RS-1 data users with enhanced capabilities. RS-2 has a three-tier imaging capability, with a unique combination of payloads consisting of three solid-state cameras, viz., a high resolution Linear Imaging Self Scanning Sensor - LISS-IV, and two medium resolution cameras namely Linear Imaging Self Scanning Sensor - LISS-III and an Advanced Wide Field Sensor- AWiFS. LISS-3 and AWIFS sensors operating at a spatial resolution of 23.5 & 56m respectively have similar bands in green (520-590 nm), red (620-680 nm), NIR (770-860 nm) and SWIR (1550-1700 nm) spectral regions. AWIFS and LISS 3 sensor covers a swath of 141 and 740 km respectively. To cover this wide swath, the AWiFS camera is split into two separate electro-optic modules, AWiFS-A and AWiFS-B.

2.2 Atmospheric Characterization Data

The aerosol information was derived from INSAT 3D AOD images (3DIMG_L2G_AOD) satellite products at a resolution of 0.1° on a half-hourly basis, while total columnar water vapour and ozone information comes from MODIS joint atmospheric products (MOD07_L2) at a resolution of 0.05°. As composting techniques can better represent the atmospheric profiles at particular location than the interpolation techniques, we have adopted mean value compositing techniques (using all available images for the specified period i.e. 5 days) rather than interpolation methods for the deriving parameter values at places where the values were missing or are invalid due to the presence of cloud.

3. METHODOLOGY

3.1 Processing of RS-2 Imageries

Before applying the 6S code the recorded digital numbers (DN) for each band of RS-2 imagery were converted to radiance using equation (1)

$$R = \frac{DN * sat.rad}{4095} \qquad \text{---------- (1)}$$

where R is observed radiance (mW/cm^2 sr μm) and sat. rad is the saturation radiance value. 6S correction code requires the geometrical parameters like the Sun and view, zenith and azimuth angles. The sun angles (both zenith and azimuth) were derived from the lat-long value, date of pass, and scene centre time using standard formulas. The view zenith and azimuth of both the sensors were computed from the information provided in the meta data of level-1 radiometric products. Both sun and view angles were computed on per pixel basis.

3.2 Generation of Per Pixel SR Values

The atmospheric correction tool developed for the atmospheric correction (ACT-RS2) of RS-2 LISS -3 and AWIFS imageries is based on java platform. Snapshot of the ACT-RS2 tool is displayed in Figure 1.

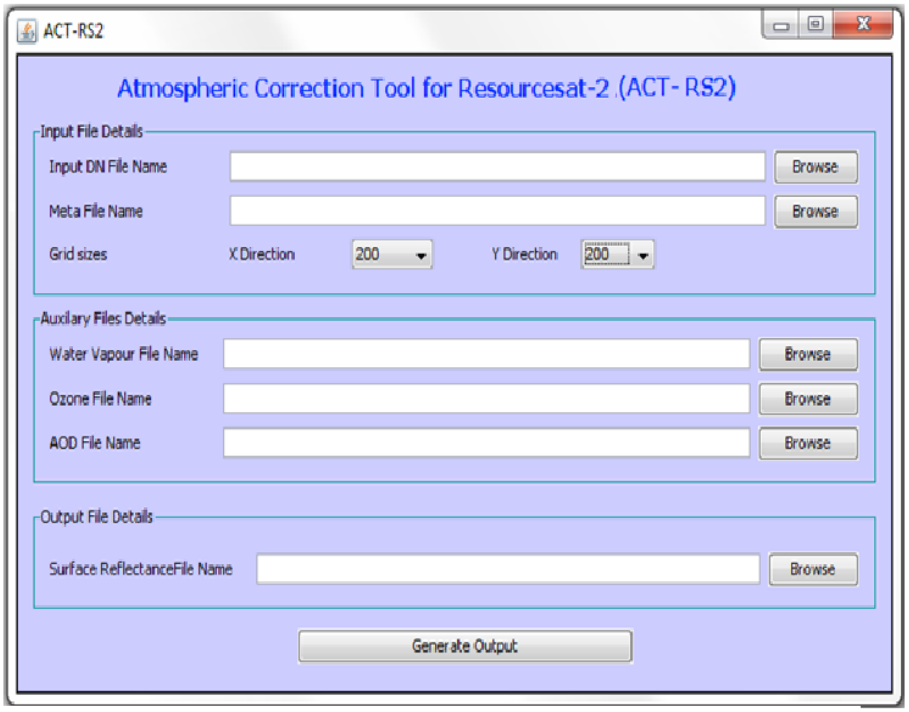

Figure 1 Snapshot of GUI developed for atmospheric correction of RS2 data

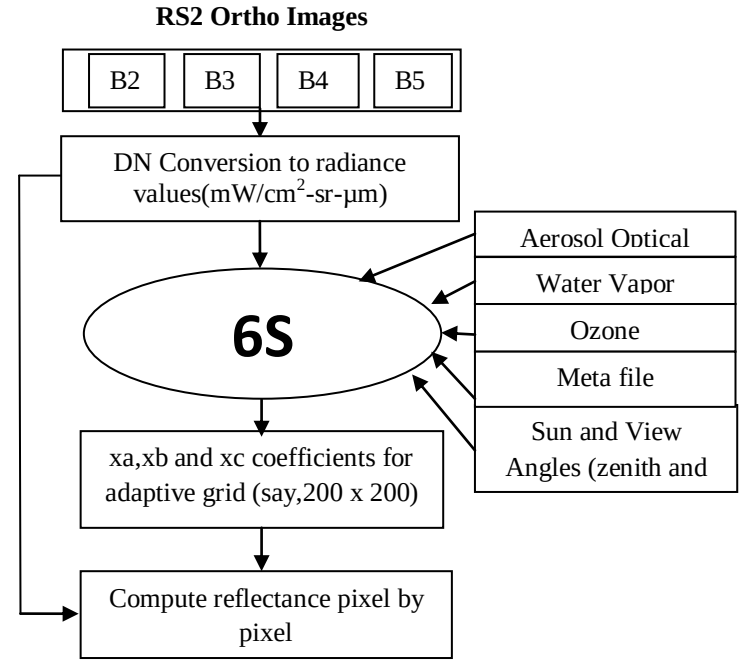

Figure 2 Flowchart depicting the atmospheric correction procedure

Using the above mentioned inputs, the 6S code was used to obtain the correction coefficients which are further used to derive the SR from the measured radiance values. For each input file the 6S code generates three correction coefficients namely xa, xb and xc. The equation to obtain SR (ρ_s) from these correction coefficients is given by (2)

$$\rho_s = (xa * L - xb)/[1.0 + xc\,(xa * L - xc)] \qquad \text{------- (2)}$$

where xa, xb and xc are the coefficients obtained from the 6S model, where, xa is the inverse of the transmittance and xb is the scattering term of the atmosphere and xc is the reflectance of the atmosphere for isotropic light entering the base of the atmosphere (Tachiri K, 2005). The number of times the 6S code is called for the generation of surface reflectance products typically depends on the grid size. The software provides an option for 3 flexible grid sizes namely, 100 X 100, 200 x 200 or 300x 300. The correction coefficients are stored as an image of 3 layers (xa, xb and xc). Finally surface reflectance was calculated pixel by pixel using the output coefficients, by applying the same values of output coefficients for all the pixels falling in the same grid. The output coefficients are computed for each band. The flowchart in Figure (2) illustrates the procedure followed to arrive at the surface reflectance products.

4. RESULTS AND DISCUSSIONS

To determine the effects of atmospheric correction, a visual comparison of ROIs extracted from TOA and surface reflectance images from LISS 3 and AWiFS sensors were undertaken with false-colour images. The TOA (Figure 3(A) &3(C)) and surface reflectance (Figure 3(B) & 3(D)) images appear quite different: there is less visual contrast in TOA reflectance due to the impact of the atmosphere

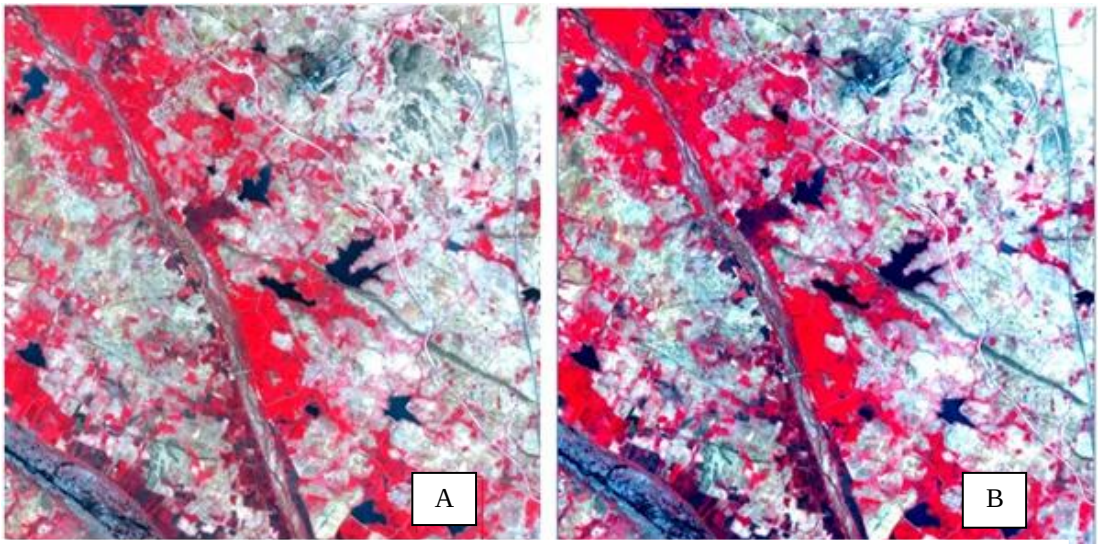

Figure 3A&B Color composite of LISS-3 ROI band3 (R), band2 (G), band1 imagery acquired on 16Feb2016 for path 100_61 (A) before and (B) after atmospheric correction

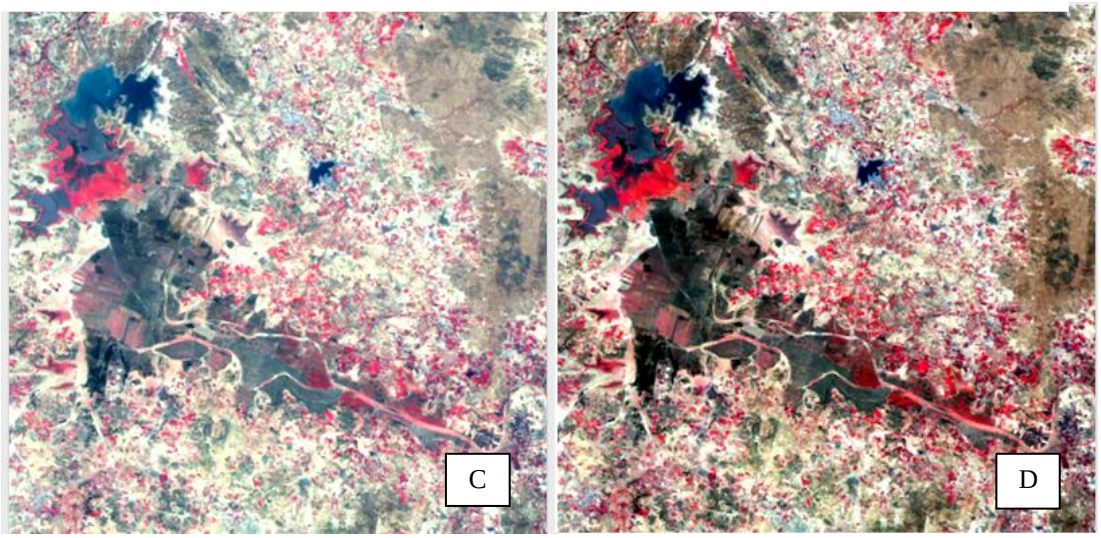

Figure 3C&D Color composite of AWiFS ROI band3 (R), band2 (G), band1 imagery acquired on 16Feb2016 for path 100_61 (C) before and (D) after atmospheric correction

4.1 Inter-Sensor Validation

The SR images generated using the ACTRS2 software were validated with L8 OLI SR images acquired over the same period with a margin of 3 days on either side. AWiFS and LISS-3 data are comparable with 30m resolution of L8 OLI data. L8 OLI SR products were aggregated using nearest neighbor interpolation techniques to match the resolution of LISS-3 and AWIFS. Validations were carried with AWiFS and LISS-3 scenes acquired during the period Jan 2015- Jan 2016. Data was selected so as to include a wide variety of target reflectance from lesser reflecting water targets to highly reflecting river sand. Table 1 compares the bandwidth of RS2 and OLI.

Table1: The 4 multispectral bands of the RS-2 LISS 3 and AWiFS sensors and the corresponding L8

	Landsat8 OLI BW in µm	RS2 AWIFS/LISS 3BW in µm
Green band	Band3 0.53-0.59	Band2 0.52-0.59
Red band	Band4 0.64-0.67	Band3 0.62-0.68
NIR band	Band5 0.85-0.88	Band4 0. 77-86
SWIR band	Band6 1.57-1.65	Band5 1.55-1.70

A scatter plot is produced for each individual RS-2 LISS-3 and AWIFS band with L8 OLI band for various targets. A linear regression (black line) was then calculated to represent the differences in surface reflectance between L8 and RS-2 pixels. In each scatter plot L8 OLI SR values are represented on the x-axis; RS-2 SR values are represented on the y-axis; respectively. The 1:1 line (red line) is also added to each chart as in figure 4 & 5. R^2 values are observed to be greater than 98% for all the four bands in both the sensors. Root mean square error values (RMSE) (Sqrt($\sum(\rho_{L8} - \rho_{L3})^2/N$)) for visible bands were found to be lower as compared to infrared bands.

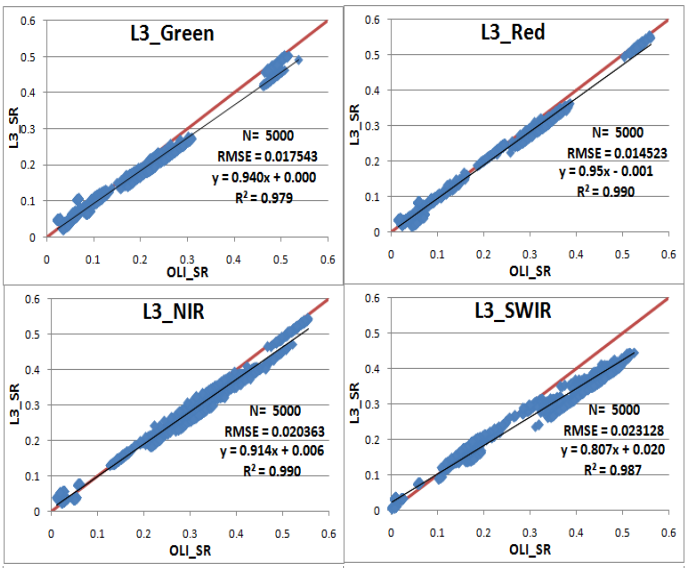

Figure 4. Scatter plot computed for SR values of different targets between LISS-3 and OLI

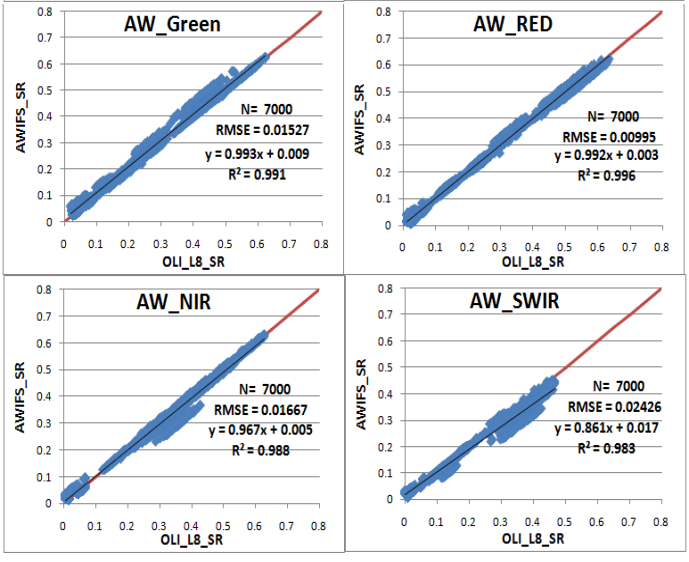

Figure 5. Scatter plot computed for SR values of different targets between AWiFS and OLI

4.2 Comparison of Histogram

The difference is further quantitatively estimated by comparing the histogram of both corrected and uncorrected images. The histograms of uncorrected TOA reflectance compared with the corresponding atmospherically corrected for AWiFS image (99_59_A_16thfeb2015) for each spectral band (Figure 6). It is evident that the atmospheric correction has smoothened all the four histograms. The values of surface reflectance were lower than the TOA reflectance in visible bands. It shows that the TOA reflectances are corrected for the scattering effects which are predominant in these wavelengths. The impact of the atmosphere on the SWIR bands was obviously less than for the other bands. Also spread in histogram of surface reflectance image confirms a contrast improvement of the atmospherically corrected image by reducing the response of the lower reflecting targets(< 0.15%) and increase in reflectance of higher reflecting targets (> 0.15%) .

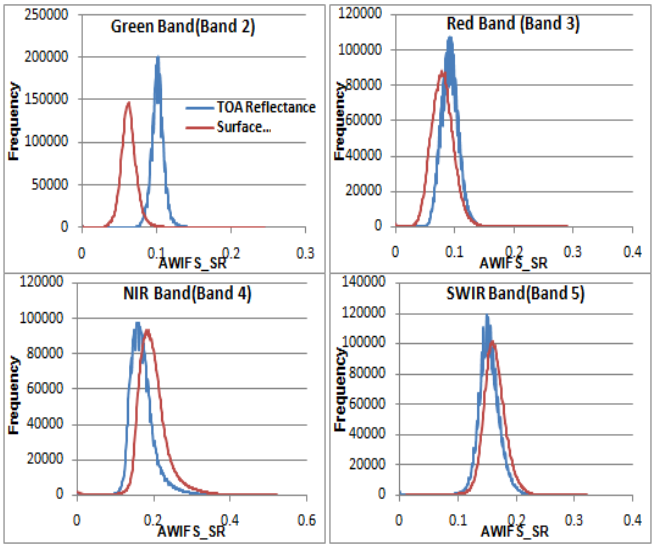

Figure 6. Histograms of reflectance in AWIFS images before and after atmospheric correction

4.3 Validation with Field Spectrometer Data

Scatter plots between the LISS-3 surface reflectance and spectroradiometer measurements acquired on five different dates in the year 2015 over different targets of the IMGOES (The Integrated Multi-mission Ground Segment for Earth Observation) calibration-validation site (in NRSC) confirms that LISS-3 SR are consistent with spectroradiometer readings(Figure.7) and AWiFS Surface reflectance data was compared with ground measured spectroradiometer data over Thar Desert area. Ground data over Thar Desert were collected during the following months: Nov'11, Dec'11 and Dec'12(Figure. 8)

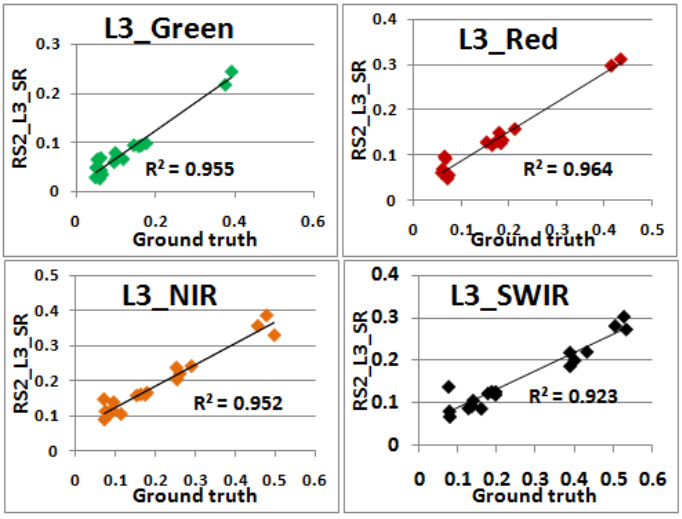

Figure 7. LISS-3 SR validated with aggregated spectroradiometer readings acquired on four dates (Jan 28, Nov 12, Dec 25, Dec 30 of 2015)

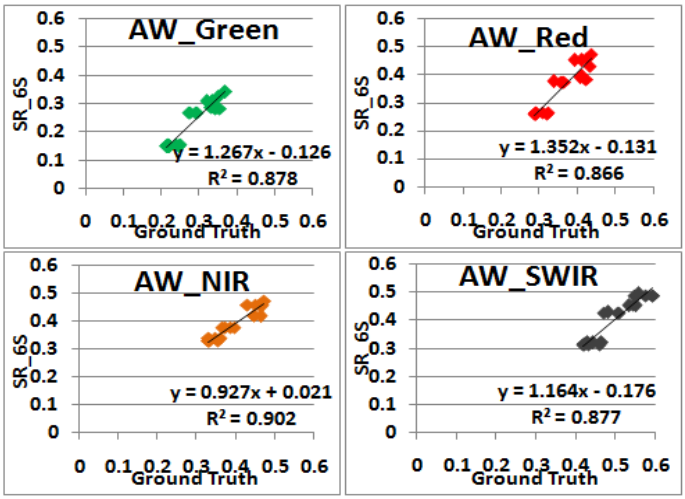

Figure 8. AWIFS SR validated with aggregated spectroradiometer readings acquired over Thar Desert.

The SR values found to be very well correlated with ground measured spectral values for LISS 3 sensor with R^2 values near to 95%. The AWiFS SR values were found to be slightly higher than the ground measured values with R^2 value of more than 85%.

4.4 Application of Atmospheric Correction

In order to evaluate the effect of atmospheric correction in the generation of information products, the NDVI values of vegetated pixels before and after atmospheric correction in AWiFS images are compared. The result of the analysis is shown in Figure 9. It is conspicuous from the slope greater than one and positive offset that the atmospheric correction has increased the NDVI values. The observed pattern matches to already reported fact the NDVI calculated from apparent reflectance is the lowest while the NDVI derived from surface reflectance values are much higher (Song and Woodcock, 2003). Atmospheric effects tend to reduce the NDVI (Pinty and Verstraete, 1992) and NDVI derived from surface reflectance products can better account for the vegetation vigor. The effect is further illustrated on LISS-3 NDVI images (Figure.10).

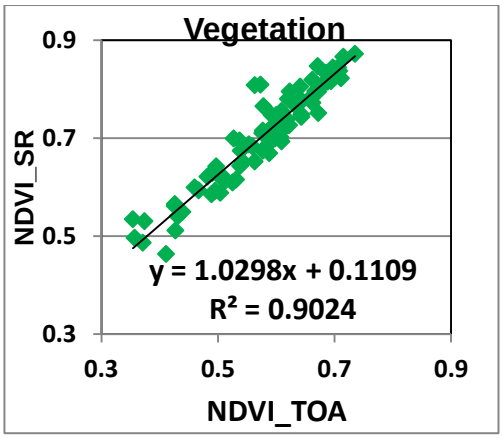

Figure 9. Scatter plot of NDVI values before and after atmospheric correction

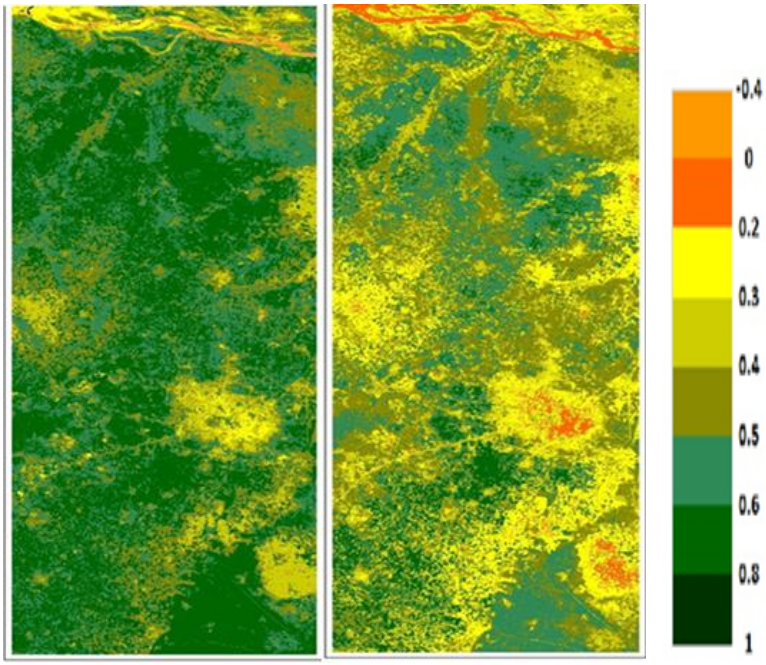

Figure 10. NDVI images after (left) and before (right) atmospheric correction for LISS -3 image acquired on 05 Oct 2015 for Punjab region.

5. CONCLUSIONS

The per-pixel atmospheric correction method employed for RS-2 sensors can account for atmospheric variation within each scene and yield a surface reflectance product of higher accuracy. The visual and histograms analysis of the images before and after the correction shows that the image corrected by 6S model increased the spectral contrast between ground targets and obtained wider distribution of reflectance carrying more information. The results of validation with multi date ground and contemporaneous satellite measurements show a good correlation with retrieved surface reflectance products. The band width of the OLI sensor is slightly different to that of RS-2 sensor especially for the NIR bands. This accounts for the slight differences in the reflectance measurements in the NIR band of both sensors. The SWIR band has larger deviation in SR values as compared to OLI SR values at higher reflectance values, which may be due to inherent short comings like the band saturation at higher reflectance in RS2 sensors. The impact of atmospheric correction on the quantitative retrieval of information from remote sensing images is illustrated using NDVI image as an example

ACKOWLEDGEMENT

We sincerely thank Director NRSC Dr. Y.V.N. Krishna Murthy for his support and encouragement. Technical discussions held with Dr. Shesha Sai, Dr. K. Sreenivas, Dr. C.S Murthy and Dr. M. Venkata Ramana , NRSC are sincerely acknowledged. We thank the Data & Product Quality Evaluation Division, NRSC and Dr. S.S.Srivastava Signal and Image Processing group, Space Application Centre for providing us the field spectrometer data used for validating surface reflectance products.

REFERENCES

Diner, D.J., Martonchik, J.V., Kahn, R.A., Pinty, B., Gobron, N., Nelson, D.L., Holben, B.N., 2004. Using angular and spectral shape similarity constraints to improve MISR aerosol and surface retrievals over land. Remote Sensing of Environment, 94 (2), pp. 155-171

Gordon, H R., 1997. Atmospheric correction of ocean color imagery in the earth observing system era**.** Journal of Geophysical Research-Atmospheres, 102 (D14), pp. 17081-17106.

Liang, S.,(2004). Quantitative Remote Sensing of Land Surfaces. Wiley-Interscience pp.196-226.

Pinty, B., Verstraete, M M., 1992 GEMI: "A nonlinear index to monitor global vegetation from satellites". Vegetatio 101(1), pp. 15-20.

Prabir Kumar Das, S.V.C. Kameswara Rao, G. Sravan Kumar and M. V. R Seshasai 2015." Retrival of bio-physical parameters for cotton and rice crop using Resourcesat-2 AWiFS data in Nalgonda district, Andhra Pradesh", Indian Journal of Spatial Science

Song, C., Woodcock, E.C., 2003. Monitoring forest succession with multitemporal Landsat images : factors of uncertainty. IEEE Trans. Geosci. Remote Sens, 41(11), pp.2557 -2567

Tachiri, K., 2005. Calculating NDVI for NOAA/AVHRR data after atmospheric correction for extensive images using 6S code: A case study in the Marsabit District, Kenya, ISPRS Journal of Photogrammetry & Remote Sensing, 59(3), pp. 103–114.

Vermote, E. F., El Saleous, N. Z. and Justice, C. O., 2002. "Atmospheric Correction of MODIS Data in the Visible to Middle Infrared: First Results." Remote Sensing of Environment, 83 (1–2), pp. 97–111.

Yong, Hu., Liangyun Liu., Lingling Liu., Dailiang Peng., Quanjun Jiao., and Hao Zhang., 2014. A Landsat-5 Atmospheric Correction Based on MODIS Atmosphere products and 6S Model. IEEE Journal of Selected topics in applied earth observations and remote sensing, Vol.7 (5) pp.1609-1615.